Numerical Simulation of Swirl Atomizers for Liquid Propellant Rocket Engines

Brunno Barreto Vasques, brunno04017@yahoo.com
Wladimyr Mattos C. Dourado, wladimyr@iae.br
Instituto de Aeronáutica e Espaço, Praça Marechal Eduardo Gomes, 50, 12228-904 São José dos Campos, Brasil

Marcio Teixeira de Mendonça, marcio@ita.br
Instituto Tecnológico de Aeronáutica, Praça Marechal Eduardo Gomes, 50, 12228-900 São José dos Campos, Brasil

Abstract. *Numerical simulations of a 5 kN-thrust rocket engine swirl atomizer were performed using an open source CFD code. Theoretical predictions of discharge coefficient, spray cone angle and liquid film thickness were obtained for both the oxidizer and fuel elements. The governing equations are solved based on the laminar volume of fluid (VOF) interface capturing method. Work is currently in progress to evaluate Reynolds Averaged (RANS) and Large Eddy (LES) turbulent numerical models. The laminar VOF model is found to agree reasonably well with analytical calculations - based on the Abramovich theory - and experimental cold flow test data. The study plays a vital role in predicting injector performance parameters as well as attempts to expand the vision for Computational Fluid Dynamics as a rocket injector design tool.*

1. INTRODUCTION

Swirl injectors have been employed in a wide variety of areas such as crop dusting, fire protection, industrial furnaces, gas turbines, diesel engines and, of course, rocket engines. Swirl atomizers are considered a low cost and reliable type of atomizer for propellant injection due to its good atomization characteristics and inherently simple geometry. Since swirl atomizers provide throttling capability (Bazarov, 1985) and high-thrust per element, they have been intensely applied in aerospace propulsion systems for over the past 60 years.

From the standpoint of operational requirements, it is highly desirable to conceive atomizers capable of producing sprays with predetermined droplet size distribution at the appropriate combustor location, thus providing an uniform heat release from the combustion process.

An important feature of swirl injectors is their intense dynamic coupling with upstream and downstream perturbations, as well as instabilities arising from the atomizer internal flow. In rocket propulsion applications, dynamic characteristics are important to predict injector performance and establish a better understanding of combustion instability phenomena related to the engine dynamic response.

The workings of a hollow-cone swirl atomizer can be explained with reference to Fig.1. It is composed mainly of tangential channels, a swirl chamber and an exit nozzle. The liquid enters the swirl chamber tangentially under the supply pressure, where due to geometry, it is caused to rotate about the center axis creating a free vortex inside the chamber. The swirl velocity obeys a constant-divided-by-radius velocity profile, which is dependent on entry conditions. This relationship between swirl velocity and radius means that the swirl velocity is highest at small radii, so much so that according to the pressure-velocity relationship of Bernoulli, the pressure there reduces to match that of the ambient medium into which the liquid is subsequently ejected. This allows the medium to enter along the axis of the atomizer to form a hollow “air" core. Thus if the liquid is discharged to the atmosphere, the radius of the air core occurs at that position where, due to the magnitude of the dynamic (velocity) head, the static pressure has become zero gauge.

The dynamic head is constant all along the surface of the air core as the pressure there is constant at a given ambient medium pressure. However, due to continuity, the axial velocity is greater in the smaller-diameter outlet than in the swirl chamber. This means that the swirl velocity on the air core in the outlet must be smaller than that on the air core in the swirl chamber. This can only be so, as the swirl is constant for any radius throughout the axial length of the atomizer, and it decreases with increasing radius, then the radius at which the static pressure equals that of the ambient medium must be greater than in the swirl chamber in order for the net velocity head be equal to the constant total pressure, given by the Bernoulli equation.

Over this description of “ideal fluid" within the swirl atomizer, there are real fluid effects. These include the effects of viscosity on the wall boundaries of the flow domain and friction losses in the inlet channels, which will act to retard the flow of the liquid and effectively alter the perceived atomizer dimensions from the ideal fluid scenario. In particular, in reducing the diameter of the outlet orifice. Also, turbulence effects will alter the flow regime from the ideal case. This poses significant difficulties to the solution of atomizer flow. A handful of analytical models, experimental and numerical methods have been employed in an attempt to describe the flow behavior inside swirl injectors.

The most notable efforts in the West to model the flow inside swirl atomizers were published by G. Taylor (1948) and again a few years later by Giffen and Muraszew (1953). In the Soviet Union, the works of V. A. Glushko in 1932 and

G. N. Abramovich (1946) in the late 40's set a standard methodology for swirl injector design. Recently, J. J. Chinn (2009) revisited swirl injector theory with reference to the *principle of maximum flow* to elucidate and compare the analyses of Giffen and Muraszew (1953), G. N. Abramovich (1944) and G. Taylor (1948). This study concluded that the mentioned authors have all conceived of essentially the same inviscid formulation for pressure swirl atomizer internal flow.

The effect of swirler geometric parameters on spray characteristics has been experimentally investigated by Kim et al. (2007) and more recently, by Chu et al. (2008). Although not all geometric parameters can be investigated, these experimental studies contribute to validate the usefulness of most analytical models.

Attempts were also made numerically to explore the underlying mechanisms of fluid injection and combustion. Recently, an interesting investigation was conducted by Hinckel et al. (2008). The purpose of this work was to determine the accuracy of the original well-known Abramovich solution (Vasiliev et al., 1993) and other non-ideal flow solutions. The numerical solution was relied upon a commercial CFD package and the standard $\kappa - \epsilon$ turbulence model. The CFD model agreed qualitatively well with the available experimental results, and discrepancies were attributed to the large mass flows employed in the experiments. More recently, Park and Heister (2010) simulated the atomization processes in a pressure-swirl atomizer via axisymmetric boundary element method. The implementation provided a first-principles capability to simulate drop size distributions for low viscosity fluids.

2. THE ABRAMOVICH ANALYTICAL MODEL

Modeling the inviscid flow physics of a swirl injector represents a great challenge to swirl injector design. The fluid enters the swirl chamber off axis at the velocity W_{in}, forms a circumferential swirling flow, exhausts at the axial velocity W_{an} through the nozzle and finally establish a near-conic sheet in the mixture-formation zone. Ideally, the liquid sheet has the shape of a hyperboloid of revolution. The spray angle is determined by the ratio of tangential and axial velocities at the nozzle exit, as given by Equation (1):

$$\alpha = \arctan\left(\frac{W_{un}}{W_{an}}\right) \tag{1}$$

where α is the spray cone half angle and W_{un} and W_{an} are the tangential and axial components of velocity at nozzle exit, respectively.

Several models exist to describe the relationship between the atomizer geometry and the flow characteristics of the swirl injector. Each of these models made the following assumptions:

- Incompressible flow;
- Inviscid flow;
- Gravity and surface effects are negligible;
- Angular momentum is constant.

The second assumption translates into irrotational flow. In other words, $\nabla \times \vec{W} = \vec{0}$. This condition is used to describe the conservation of angular momentum inside the atomizer:

$$rW_u = constant \tag{2}$$

or, between the inlet channels and other arbitrary point in the injector,

$$W_{in}R_{in} = W_u r \tag{3}$$

The liquid potential energy in the form of pressure drop across the injector is fully converted to kinetic energy. Hence, the total liquid flow velocity is:

$$W = \sqrt{\frac{2}{\rho}\Delta p_{inj}} = \sqrt{W_u^2 + W_a^2 + W_r^2} \tag{4}$$

where Δp_{inj} is the pressure drop across the injector.

The radial component of velocity, W_r is assumed negligible, hence

$$W = \sqrt{W_{uk}^2 + W_{ak}^2} = \sqrt{W_{un}^2 + W_{an}^2} = W_{uo} \tag{5}$$

The subscripts o, k and n denote the conditions at the injector head end, vortex chamber and nozzle, respectively. At the injector head end, $W_a = 0$. The circumferential component of the liquid velocity W_{uo} is maximum and the radius of liquid-vortex surface, on the contrary, is minimum. In the vortex chamber, the axial velocity W_{ak} is positive and the circumferential velocity is W_{uk} is smaller than W_{uo}, giving $r_{gk} > r_{go}$. In the nozzle, the smaller liquid passage area leads to an increase of the axial velocity W_{an} and a decrease of W_{un}, giving $r_{gn} > r_{gk}$. Finally, at the nozzle exit, the centrifugal force arising from the swirling motion acts as a velocity head, leading to an additional increase of the axial velocity and subsequently an increase of the liquid-surface radius.

Since a gas core must be present, otherwise, from Equation (2), the angular velocity would be *infinite*, the liquid will not fully occupy the entire injector. Thus, a *coefficient of useful cross section*, φ, that relates the area filled by the liquid to the nozzle area, can be defined:

$$\varphi = \frac{\pi(r_n^2 - r_{gn}^2)}{\pi r_n^2} = 1 - \frac{r_{gn}^2}{r_n^2} \tag{6}$$

Various geometric parameters can be correlated to form a non-dimensional *geometrical characteristic parameter*, K, defined as:

$$K = \frac{R_{in} r_n}{n r_{in}^2} \tag{7}$$

where R_{in} is radial location of the tangential passages, r_n is the nozzle radius, n is the number of tangential channels and r_{in} is the radius of the tangential inlet passage. The *contraction ratio*, C, relates the radial location of inlet channels to the nozzle radius:

$$C = \frac{R_{in}}{r_n} \tag{8}$$

The mass flow rate through the atomizer can be obtained in terms of the non-dimensional injector parameters:

$$\dot{m}_{inj} = \frac{\pi r_n^2}{\sqrt{\frac{1}{\varphi^2} + \frac{K^2}{1-\varphi}}} \sqrt{2\rho\Delta p_{inj}} \tag{9}$$

Equation (9) may also be written as:

$$\dot{m}_{inj} = \mu_{inj} A_n \sqrt{2\rho\Delta p_{inj}} \tag{10}$$

where the A_n is the atomizer nozzle area. The discharge coefficient, μ_{inj}, is defined, for the inviscid flow in a swirl injector, as:

$$\mu_{inj} = \frac{1}{\sqrt{\frac{1}{\varphi^2} + \frac{K^2}{1-\varphi}}} \tag{11}$$

G. N. Abramovich (1946) noted that it is clear from Equation (11) that the discharge coefficient as a function of φ has small values for both small and large values of φ, passing through a maximum. As a result, a maximum value of K is observed, indicating the existence of the maximum flow rate for a given K. In accordance with the Principle of Maximum Flow (Abramovich, G. N.,1944), one may find that

$$K = \frac{(1-\varphi)\sqrt{2}}{\varphi\sqrt{\varphi}} \tag{12}$$

Hence, from Equation (11) the maximum discharge coefficient is

$$\mu_{inj} = \frac{\varphi\sqrt{\varphi}}{\sqrt{2-\varphi}} \tag{13}$$

and the average inviscid spray angle, $\overline{\alpha}$, can be written as:

$$\overline{\alpha} = \arctan\left\{\frac{(1-\varphi)\sqrt{8}}{\left[\left(1+\sqrt{1-\varphi}\right)\sqrt{\varphi}\right]}\right\} \tag{14}$$

Equations (13) and (14) reveal that, under the assumptions made, the discharge coefficient and spray cone angle are simply determined by the geometric characteristics and does not depend on the operating conditions of the atomizer.

Fluid viscosity and friction losses may be incorporated in Eqs. (11) and (14) by adding a momentum loss coefficient, ψ, and a resistance coefficient, ξ_{inj}, as follows:

$$\mu_{inj} = \frac{1}{\sqrt{\frac{2-\varphi}{\varphi^3} + \xi_{inj}\frac{K^2}{C^2}}} \tag{15}$$

and

$$\overline{\alpha} = \arcsin\left[\frac{2\mu_{inj}\left(\psi K\right)}{\left(1+\sqrt{1-\varphi}\right)\sqrt{1-\xi_{inj}\mu_{inj}^2\frac{K^2}{C^2}}}\right] \tag{16}$$

For low-viscosity fluids, ψ is usually close to unit. The resistance coefficient is obtained from test data, or by use of tables available in the literature (Vasiliev et al., 1993).

3. NUMERICAL SOLUTION

The CFD tool employed was the OpenFOAM version 1.6. OpenFOAM is a *C++ library* used primarily to create executables, known as *applications*. The applications are divided into two categories: *solvers*, assigned to actually solve a specific problem in continuum mechanics, and *utilities*, designed to provide a wide range of functionalities regarding pre- and post-processing. Being an *open source code*, OpenFOAM allows the creation of new solvers and utilities at user's discretion, as long as some pre-requisite knowledge of the underlying method, physics and programming techniques are concerned.

3.1 Governing equations

The solutions presented in this paper implements the laminar *volume of fluid* (VOF) equations. In the VOF capturing interface method, one momentum equation and one continuity equation are solved. These equations are the same for both fases, the physical properties of one fluid being calculated as a weighted-average based on the volume fraction of the two fluids in one cell. The momentum equation can be written as:

$$\frac{\partial\left(\rho\vec{W}\right)}{\partial t} + \nabla\bullet\left(\rho\vec{W}\vec{W}\right) - \nabla\bullet\mu\nabla\vec{W} - \rho\vec{g} = -\nabla p - \vec{F}_s \tag{17}$$

where μ is the dynamic viscosity and $\vec{F}_s$ is the surface tension force. The continuity equation assumes the form

$$\nabla\bullet\vec{W} = 0 \tag{18}$$

The volume of fluid in a cell is computed as $F_{vol} = \gamma V_{cell}$, where V_{cell} is the volume of a computational cell and γ is the fluid fraction in a cell. The values of γ range from 0 to 1. Therefore, a cell completely filled with fluid is represented by $\gamma = 1$; on the other hand, the void phase indicates a γ value equal to 0. At the interface γ assumes any value between 0 and 1. The scalar function γ is computed from a separate transport equation given by

$$\frac{\partial\gamma}{\partial t} + \nabla\bullet\left(\gamma\vec{W}\right) = 0 \tag{19}$$

In OpenFOAM, the necessary compression of the surface is achieved by introducing an extra artificial compression term into Eq. (19) as follows:

$$\frac{\partial\gamma}{\partial t} + \nabla\bullet\left(\gamma\vec{W}\right) + \nabla\bullet\left[\gamma\left(1-\gamma\right)\vec{U}_r\right] = 0 \tag{20}$$

where U_r is a velocity field suitable to compress the interface. This artificial term is active only in the interface region due to the term $\gamma\,(1-\gamma)$.

Fluid properties at any point in the domain are calculated as the weighted-average of the volume of fluid of the two fluids as:

$$\rho = \gamma\rho_1 + (1-\gamma)\,\rho_2 \tag{21}$$

$$\mu = \gamma\mu_1 + (1-\gamma)\,\mu_2 \tag{22}$$

where the subscripts 1 and 2 indicate the phases involved (a liquid and a gas, for example).

The surface tension F_s is computed as:

$$\vec{F}_s = \sigma\kappa\,(x)\,\vec{n} \tag{23}$$

where $\vec{n}$ is a unit vector normal to the interface that can be calculated as

$$\vec{n} = \frac{\nabla\gamma}{|\nabla\gamma|} \tag{24}$$

and κ is the curvature of the interface given by

$$\kappa\,(x) = \nabla \bullet \vec{n} \tag{25}$$

Equations (25) through (33) are implemented in the interFoam solver, through a pressure-implicit split-operator (PISO) algorithm, present in the OpenFOAM applications directory.

3.2 Fluid domain and boundary conditions

The solution was obtained for both the fuel and oxidizer core elements. The initial condition is defined by filling the entire fluid domain with stationary liquid. The imposed boundary conditions were a total pressure of 5 [bar] at the inlet and a static pressure of 1 [bar] at the outlet, thus giving the nominal 4 [bar] pressure drop.

The discretization of the fluid domain is accomplished by a powerful, yet not flawless, OpenFOAM utility. This tool generates three-dimensional grids containing primarily hexahedra and split-hexahedra automatically from surface geometries in Stereolithography (STL) format. Combined with adaptive mesh refinement, the mesh generation process is made easier. The final LOX injector mesh consisting of approximately 2.5 million points, is shown Fig. (1).

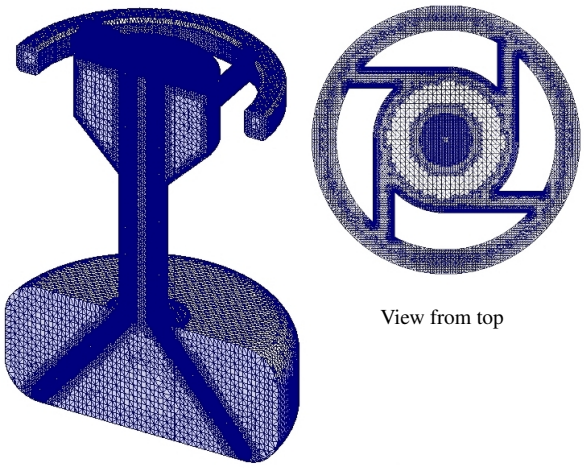

Figure 1. Final mesh obtained for the LOX atomizer.

3.3 Results

Cold flow solutions were pursued for both swirlers at the prescribed boundary conditions. Water was used as the simulant liquid and the gaseous phase is air. Fluid properties are summarily presented in Tab. 1. The velocity and

Table 1. Fluid Properties (Kit and Evered, 1960)

Water properties	Units	Value
Kinematic viscosity	$[m^2 s^{-1}]$	1.0×10^{-6}
Density	$[kg\,m^{-3}]$	1.0×10^{3}
Air properties		
Kinematic viscosity	$[m^2 s^{-1}]$	1.48×10^{-5}
Density	$[kg\,m^{-3}]$	1.0
Properties of both phases		
Surface tension	$[Nm^{-1}]$	0.07

thickness of the liquid film at the atomizer outlet, are of interest because they govern the breakup of the film. In both cases, especially in the LOX simulation, the interface between the liquid and gas phases become unsteady, displaying waves of small amplitude along its surface. The waves originate at the top of the atomizer, on the stagnation point on the wall, and propagate toward the exit, see Fig. 2b. The stagnation point leads to the formation of a crest at the fuel injector head end, as shown in Fig. 2a. The resulting flows are of highly three-dimensional character, where the air core is rotating, generating a spiraling disturbance on its surface.

Velocity components obtained in the simulations are depicted in Fig. 3a and Fig. 4a. Figures 3b and 4b represent the axial component of velocity across atomizer swirl chamber. As expected, their magnitude remained approximately constant throughout a fixed injector cross section. Analytical internal flow solutions show that the tangential velocity obeys a $1/r$ velocity profile. This is also the case for the numerical simulations, as represented by Fig. 3c and Fig. 4c. It was also observed that the tangential velocity is essentially independent of the axial position. As mentioned earlier, the Abramovich analytical solution assumes null radial velocity across the liquid film. From this statement, part of his model is developed. The CFD solution shows good agreement with this condition as represented by Fig. 4d and Fig. 4d.

Perhaps the most important performance parameter is the atomizer discharge coefficient. Preliminary results based on

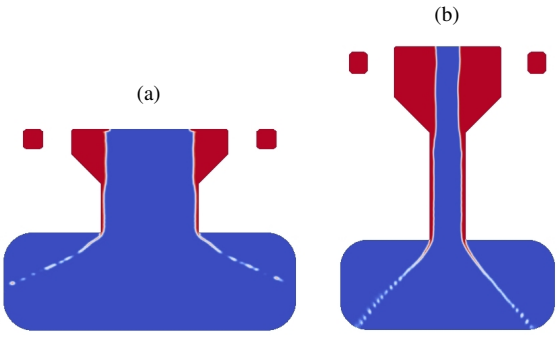

Figure 2. Phase fraction for the fuel (a) and oxidizer (b) atomizers.

the mass flow coefficient of both swirlers are presented in Table 2. Experimental data were obtained from previous test campaigns. Ideal and corrected analytical solutions are compared with the current numerical results as well.

Table 2. Analytical, Experimental and Numerical Evaluation of the Discharge Coefficient.

LOX atomizer			
μ_{exp}	μ_{id}/μ_{exp}	μ_{corr}/μ_{exp}	μ_{num}/μ_{exp}
0.230	0.91	0.90	0.74
Fuel atomizer			
μ_{exp}	μ_{id}/μ_{exp}	μ_{corr}/μ_{exp}	μ_{num}/μ_{exp}
0.0210	0.78	0.91	0.73

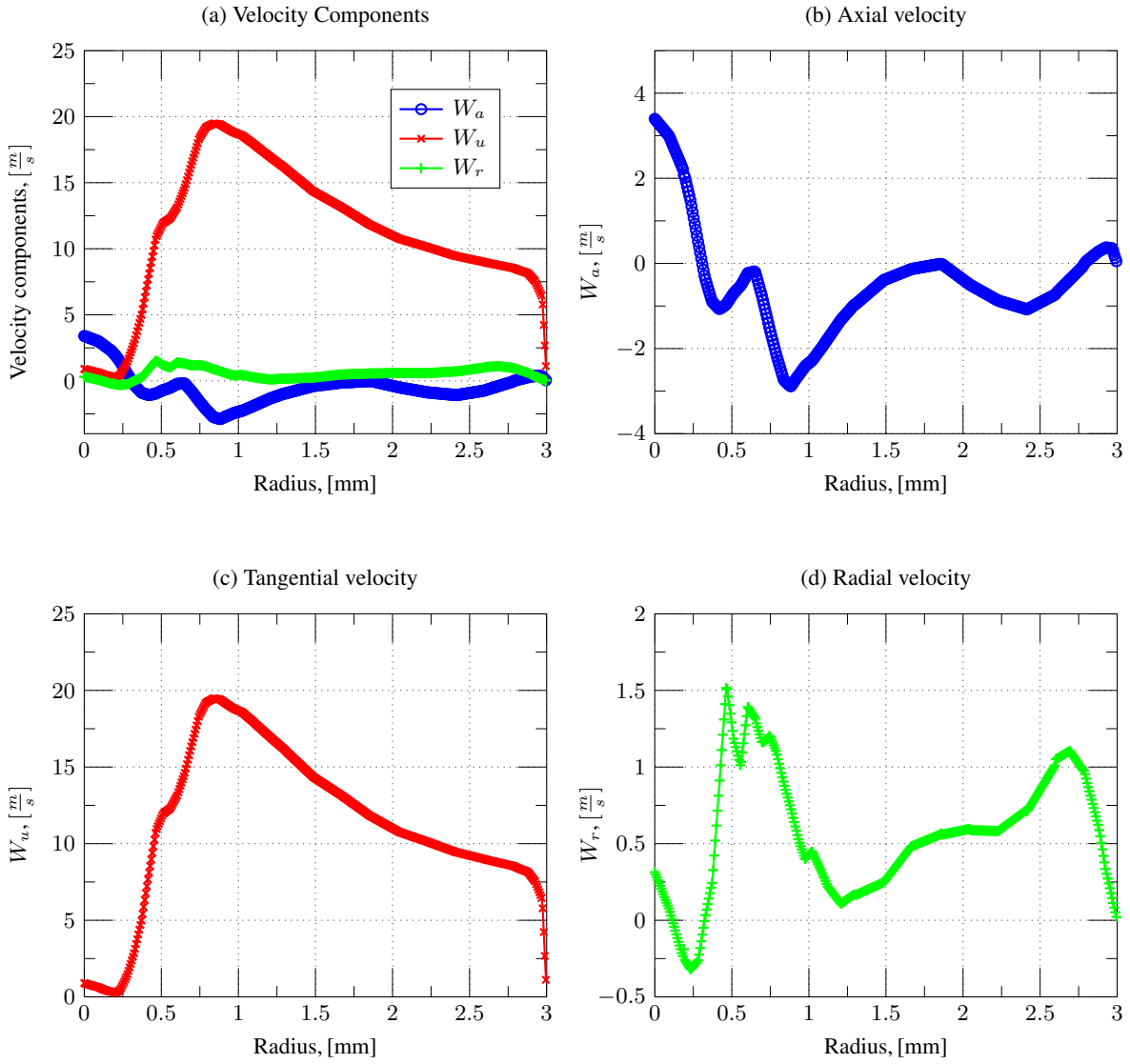

Figure 3. Velocity components at LOX swirler vortex chamber.

4. CONCLUSION

The core injection element of a 5-[kN] was evaluated numerically using an Open Source CFD code. The laminar VOF method employed represented a first step in the direction of more sophisticated turbulence models. This simplified model was able to match reasonably well the predicted performance parameters obtained from ideal and corrected analytical solutions, based on the Principle of Maximum Flow.

Discrepancies of up to 25% were observed in comparison to previous cold flow test data. Although significant, these deviations are well within those described in the available literature (Vasiliev et al., 1993). Despite that, more accurate predictions of atomizer spray cone angle, discharge coefficient and especially liquid film thickness are encouraged. This can be accomplished by use of different turbulent models and mesh refinement. Eventually, a more precise experimental setup may also be required.

Work is currently in progress to ascertain the use of these resources, in particular, through a Laser Doppler Velocimetry equipment and LES turbulence model.

5. ACKNOWLEDGEMENTS

The authors would like to thank the Division of Space Propulsion for providing the preliminary experimental results.

6. REFERENCES

Abramovich, G. N., 1944, "The Theory of Swirl Atomizers", Industrial Aerodynamics, BNT ZAGI, Moscow, Russia.

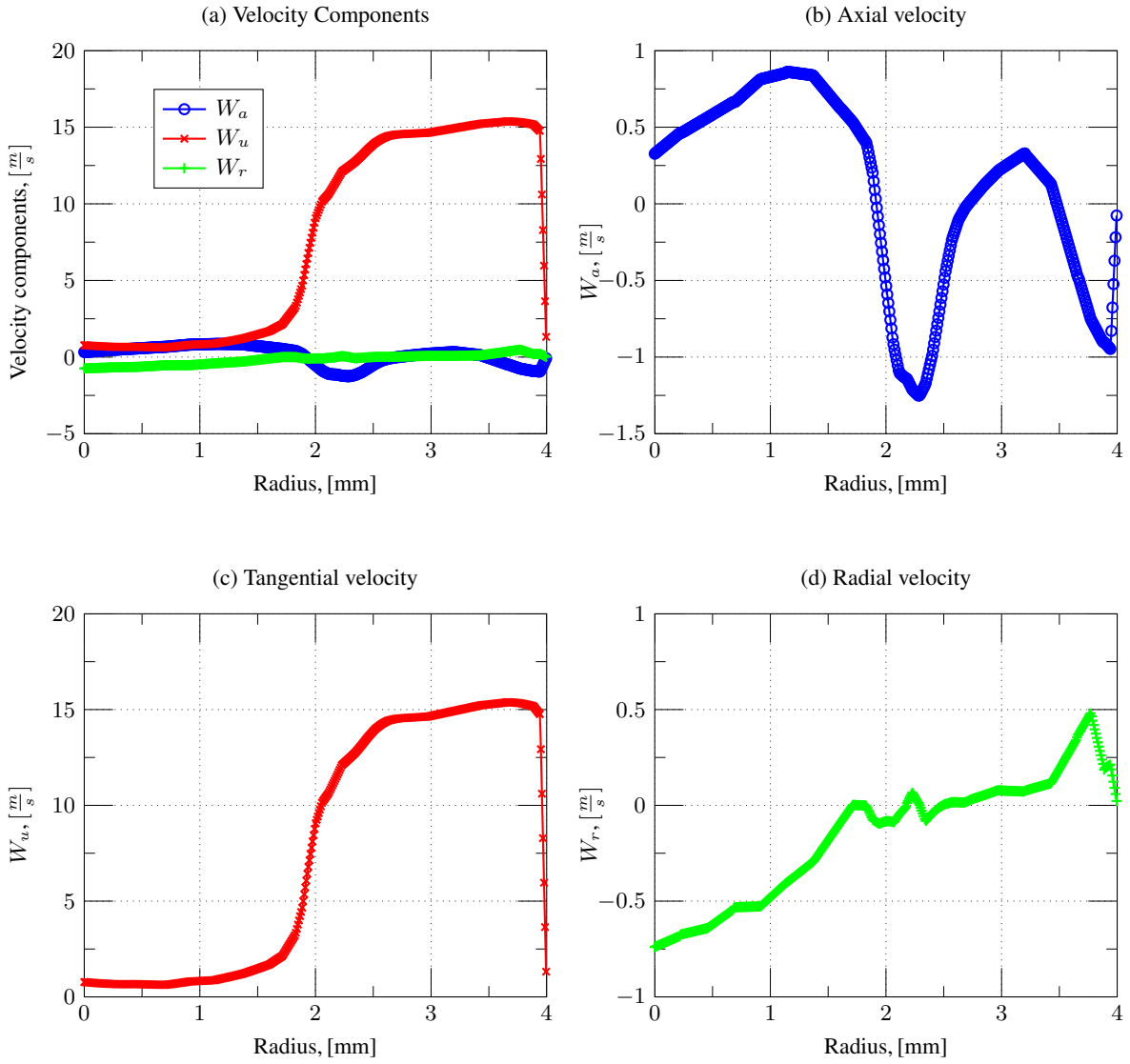

Figure 4. Velocity components at fuel injector vortex chamber.

Mikhailov, V. V. and Bazarov, V. G.,1985, "Throttlable Liquid Rocket Engines", Mashinostroyeniye Press, Moscow, Russia.

Chu, Chia-Chien and Chou, Shyan-Fu and Lin, Heng-I and Liann, Yi-Hai, 2008, "An experimental investigation of swirl atomizer sprays", Heat and Mass Transfer, Vol. 45, pp. 11-22.

Hinckel, J. N. and Villa Nova, H. F. and Bazarov, V. G., 2008, "CFD Analysis of Swirl Atomizers", 44th AIAA/ASME/SAE/ASEE Joint Propulsion Conference and Exhibit.

Giffen, E. and Muraszew, A., 1953, "Atomization of Liquid Fuels", Chapman and Hall, London.

Taylor, G., 1948, "The Mechanism of Swirl Atomizers", Proceedings of the 7th International Congress for Applied Mechanics, Vol. 2, London.

Kim, D. and Im, Ji-Hunk and Koh, H. and Yoon, Y., 2007, "Effect of Ambient Gas Density on Spray Characteristics of Swirling Liquid Sheets", Journal of Propulsion and Power, Vol. 23, No. 3, pp. 603-611.

Park, S. K. and Heister, S. D., 2010, "Nonlinear Modeling of Drop Size Distributions Produced by Pressure-Swirl Atomizers", International Journal of Multiphase Flow, Vol. 36, No. 1, pp. 1-12.

Vasiliev, A. P. and Kurpatenkov, V. M. and Kuznetsov, V. A. and Kurpatenkov, V. D. and Obelnitsky, A. M. and Poliaev, V. M. and Poliaev, B. I., 1993, "Ochnoviy Teori y racheta GRD" (in Russian), Moskwa Vischkaia Skola, Moscow, Russia.

7. Responsibility notice

The authors are the only responsible for the printed material included in this paper